ACS OMEGA

http://pubs.acs.org/journal/acsodf

Article

Prodrug Based on Ionic Liquids for Dual-Triggered Release of Thiabendazole

Wenbing Zhang, Yan Guo, Jiale Yang, Gang Tang, Jian Zhang, and Yongsong Cao*

Cite This: *ACS Omega* 2023, 8, 3484−3492

Read Online

ACCESS | Metrics & More | Article Recommendations

ABSTRACT: The application of triggered release pesticides can provide active ingredient release at required environmental conditions, reduce environmental problems, and toxicity to nontarget organisms. In this work, a novel prodrug that responds to water and enzymes as release triggers for thiabendazole was prepared. The release behaviors under different conditions, bioactivity against *Penicillium italicum*, and acute toxicity to *Danio rerio* of prodrugs were investigated. The results showed that the prodrug had remarkable water- and enzyme-triggered release properties, and the correlation coefficients (r^2) fitted by the Weibull model were all >0.99. Meanwhile, the prodrug showed improved antifungal efficacy against *Penicillium italicum* and reduced toxicity to *Danio rerio*. Overall, the prodrug developed offers an efficient way to triggered release pesticides, control fungal, and reduce the risk of harm to aquatic organisms.

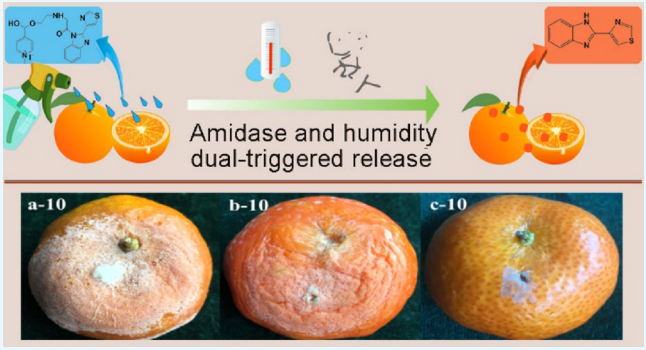

1. INTRODUCTION

The consumption of chemical pesticides applied to control pathogens, pests, and weeds has been continuously increasing in past decades.[1] It is estimated that about 90% of the pesticides are wasted via degradation, evaporation, and surface runoff, and only about 0.1% of the pesticides are effectively acted on the target organisms.[2,3] Therefore, the more efficient, safe, and green pesticide formulations are needed to be developed to reduce the risk of pesticides on food safety and ecological environments.[4−8] Encapsulation of active ingredients into appropriate carrier materials, or specially designed capsules, has been widely applied to improve the utilization rate of pesticides.[9,10] Meanwhile, carriers prevent direct exposure of pesticides to the environment, decreasing loss of evaporation and degradation.[11,12] Pesticides encapsulated in microcapsule carriers that are susceptible to release slowly in contact with environmental conditions, and the compatibility of the carriers with the environment are thought to play an important role.[13,14]

Besides, the other category of carriers that was applied in the controlled release of active ingredients is known as prodrugs.[15,16] The active ingredient is covalently bound to carriers with a trigger release mechanism by the change of the pH value, action of a specific enzyme, photo-cleavage of light with a suitable wavelength, or thermal decomposition of the prodrug.[17−20] Many pesticides contain a multitude of chemical functional groups such as hydroxy, amino, carboxylic, and cyano groups, which could be easily covalently bound with other substances.[21−23] The release of prodrugs in the form of predesigned esters or amides can be affected by the enzyme or the pH values of the release medium.[24,25]

Ionic liquid (IL) is a novel organic salt with low melting properties, marginal vapor pressure, low toxicity, and high thermal stability that have enormous potential for industrial use as "green" chemicals.[26−28] ILs have been widely used in drug applications, such as solvents for drugs, antimicrobial agents, antibiofilm agents, and drug carriers.[29,30] The structure of ILs could be modified by using different combinations of cations and anions and could be cross-linked to other chemical groups as well as modified to serve as a triggered release carrier.[31,32] IL-based drugs developed with excellent biocompatibility and long-term stability have been proved to be promising delivery carriers and should be further explored.[33]

Thiabendazole (TBZ) was first discovered to be an unusually potent broad-spectrum anthelmintic affecting gastrointestinal parasites of sheep, cattle, goats, and swine.[34] Now, it is one of the most widely applied post-harvest fungicides in controlling fungal infection in the process of fruit and vegetable storage and transportation.[35] However, the applicability of

Received: November 23, 2022
Accepted: December 28, 2022
Published: January 9, 2023

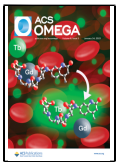

Scheme 1. Synthetic Route of Thiabendazole Prodrug (IL-TBZ)

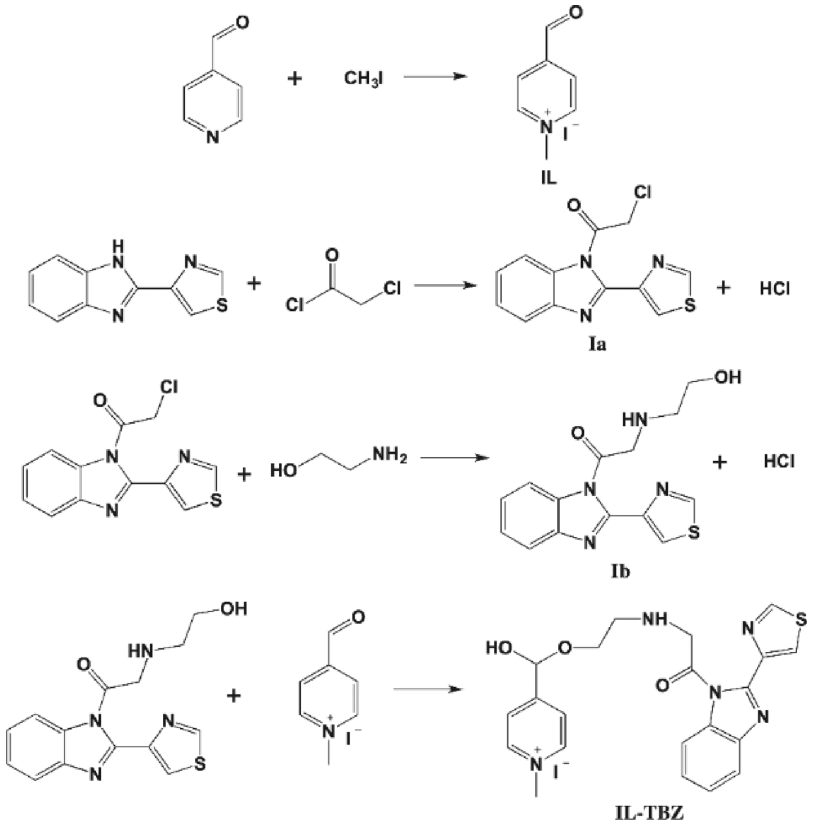

TBZ is limited for its high toxicity to aquatic fish and potential damage to the aquatic environment.[36,37]

Herein, we prepared a prodrug using IL 1-methyl-4-formylpyridinium iodide conjugated with derivatized TBZ via hemiacetal by utilizing chloroacetyl chloride and ethanolamine. The effects of humidity, pH value, and enzyme on the release behaviors were investigated, and the bioactivity and toxicity of novel conjugation were also studied.

2. EXPERIMENTAL SECTION

2.1. Materials. *2.1.1. Chemicals.* The model drug, thiabendazole (TBZ, 98%), was purchased from Alchem Pharmtech, Inc., NJ, USA. Pyridine-4-aldehyde (99%) and chloroacetyl chloride were purchased from Heowns Biochemical Technology Co., Ltd., Tianjin, China. Methyl iodide, *N*,*N*-dimethylformamide (DMF), tetrahydrofuran (THF), dichloromethane (DCM), acetonitrile, acetone, potassium carbonate, anhydrous magnesium sulfate, diethyl ether, ammonium acetate, and ethanolamine were analytical chemicals purchased from Sinopharm Chemical Reagent Co., Ltd., Shanghai, China. Amidase (~13 unit/mg; from *Citrus sinensis*) was obtained from Sigma-Aldrich (St. Louis, USA). *Penicillium italicum* strains were obtained by Seed Pathology & Fungicide Pharmacology Lab., China Agricultural University. *Danio rerio* (0.27 ± 0.05 g mean body weight and 2.65 ± 0.05 cm length) were purchased from aquarium (Tongzhou Aquarium, Beijing, China). Deionized water was applied for all reactions and treatment processes. Acetonitrile and methanol were high-performance liquid chromatography (HPLC)-grade and purchased from J.T. Baker, USA.

2.1.2. Apparatus. Identification of compounds: ^{1}H NMR spectra were determined on a Bruker Avance DPX 300 MHz NMR spectrometer (Bruker, Germany). CHN elemental analyses were performed using a 5E-CHN2000 elemental analyzer (Changsha Kaiyuan Instruments Co., Ltd., China). An HPLC system consisting of two LC-20ATvp pumps and an SPD-20Avp ultraviolet detector (Shimadzu, Japan) was used for the detection of chemicals. A Kromasil ODS C18 column (250 mm × 4.6 mm, 5 μm; DIKMA, USA) was used for separation at room temperature, and a Chromato Solution Light Chemstation for the LC system was employed to acquire and process chromatographic data. A flow rate of 1 mL min^{-1} was used with a mobile phase composition of methanol and water with 2% ammonium acetate (75/25, v/v), injecting volume 20 μL. All the solvents were filtered with 0.045 μm membrane filters.

2.2. Preparation of the Prodrug of TBZ Based on Ionic Liquids (IL-TBZ). The synthetic routes of Ia, Ib, IL, and IL-TBZ are schematically presented in Scheme 1.

2.2.1. Synthesis of Compounds Ia and Ib. First, TBZ (6 mM) and dry THF (20 mL) were added into a 100 mL three-neck flask, and chloroacetyl chloride (6 mM) in THF (10 mL) was added drop by drop for about 30 min while stirring at 0 °C. After completion of addition, potassium carbonate (10 mM) was added to the mixture, and constant stirring was done at 25 °C for additional 4 h. The reaction endpoint was confirmed by HPLC. The mixture was evaporated by a rotary evaporator, and the solid was washed extensively with deionized water and dried under vacuum at 60 °C to obtain the compound Ia.

The compound Ia (5 mM) and dry THF (20 mL) were added into a 100 mL three-neck flask, then ethanolamine (5 mM) and potassium carbonate (6 mM) were added in the reaction mixture under constant stirring for 4 h. The reaction

https://doi.org/10.1021/acsomega.2c07511
ACS Omega 2023, 8, 3484−3492

endpoint was confirmed by HPLC. The mixture was evaporated by a rotary evaporator, and the solid was washed extensively with deionized water and dried under vacuum at 60 °C to obtain the compound Ib.

2.2.2. Synthesis of ILs 1-Methyl-4-formylpyridinium Iodide (IL) and the Prodrug of TBZ (IL-TBZ). Pyridine-4-aldehyde (5 mL, 56.9 mM) and dry DCM (20 mL) were added into a 100 mL three-neck flask under constant stirring at room temperature for 30 min, then methyl iodide (7 mL, 112.4 mM) was added in the mixture under constant stirring at room temperature for 24 h. The mixture was evaporated by a rotary evaporator and dried under vacuum at 60 °C to obtain the IL.[38]

IL (2 mM), dry acetonitrile, and compound Ib (2 mM) were added in a 100 mL three-neck flask under constant stirring at room temperature for 4 h. The reaction endpoint was confirmed by TLC. The mixture was evaporated by a rotary evaporator, and the solid was washed extensively with dry diethyl ether and dried under vacuum at 60 °C to obtain the IL-TBZ.

2.2.3. 2-Chloro-1-(2-(thiazol-4-yl)-1H-benzo[d]imidazol-1-yl) ethanone, Ia. Solid; yield, 87%. Elemental analysis calcd (%) for $C_{12}H_8ClN_3OS$ (M = 277.01) C 51.90; H 2.90; N 15.13; found: C 51.88; H 2.92; N 15.23.

2.2.4. 2-((2-Hydroxyethyl)amino)-1-(2-(thiazol-4-yl)-1H-benzo[d]imidazol-1-yl) ethanone, Ib. Solid; yield, 83%; Elemental analysis calcd (%) for $C_{14}H_{14}N_4O_2S$ (M = 302.08) C 55.62; H 4.67; N 18.53; found: C 55.78; H 4.72; N 18.73.

2.2.5. 4-(Hydroxy(2-((2-oxo-2-(2-(thiazol-4-yl)-1H-benzo-[d]imidazol-1-yl) ethyl) amino) ethoxy) methyl)-1-methyl-pyridin-1-ium iodide, IL-TBZ. Solid; yield, 79%; Elemental analysis calcd (%) for $C_{21}H_{22}IN_5O_3S$ (M = 551.05) C 45.74; H 4.02; N 12.70; found: C 46.08; H 4.62; N 12.33.

2.3. HPLC Analysis of TBZ. The TBZ was determined by an HPLC system with two LC-20ATvp pumps and an SPD-M20Avp UV−vis photodiode array detector (Shimadzu, Japan) equipped with a Kromasil ODS C_{18} column (250 × 4.6 mm, 5 μm; DIKMA, USA) at 280 nm under room temperature. The mobile phase was methanol−water with 2% ammonium acetate (75:25, v/v). The flow rate was 1.0 mL min^{-1} and the injection volume was 20 μL. All the samples were filtered through a 0.45 μm membrane.

2.4. Control Release Behaviors of IL-TBZ. The release behaviors of IL-TBZ at different pH and humidity conditions were investigated by HPLC. First, 10 mg of IL-TBZ and 1 μL of amidase solution were weighted and dispersed in 100 mL of phosphate buffer saline (PBS) (pH 4.5) containing different contents of acetone (72, 62, 56, and 50%). Then, 10 mg of IL-TBZ was weighted and dispersed in 100 mL of PBS (pH 4.5, 5.5, 6.5, and 7.5) containing 62% acetone, which were used as the release medium.[39] The mixtures were incubated at a stirring speed of 100 rpm for a given time at room temperature, collected, and filtered at different intervals, and the TBZ content was determined by using HPLC to evaluate the release properties.

2.5. Release Modeling. In order to estimate the release mechanism of IL-TBZ, several common models illustrated in Table 1 have been employed to compare the various profiles and also attempted to identify the release kinetics of prodrugs. In this work, the release kinetics of IL-TBZ was calculated by applying the empirical equations listed in the table, where M_t/M_z is the percentage of TBZ release at time *t*. *k* is the constant that incorporates the characteristics of the release system and the TBZ.[40−47] The correlation coefficient (r^2) was used to identify the suitability of each fitting curve.

Table 1. Released Kinetics Models of Prodrug

release model	equations
Korsmeyer−Peppas model	$M_t/M_z = k_2 t^{k_1}$
zero-order model	$M_t/M_z = k_1 t$
first-order model	$M_t/M_z = k_2[1 - \exp(-k_1 t)]$
Hixson−Crowell model	$M_t/M_z = k_1 t + k_2 t^2 + k_3 t^3$
Weibull model	$M_t/M_z = k_3\left[1 - \exp\left(-\frac{t}{k_1}\right)^{k_2}\right]$
Higuchi model	$M_t/M_z = k_1 t^{0.5}$
logistic model	$M_t/M_z = k_3\frac{\exp(k_1 + k_2 \log t)}{1 + \exp(k_1 + k_2 \log t)}$
quadratic model	$M_t/M_z = k_1 t + k_2 t^2$

2.6. Bioactivity. Citrus fruits (*Citrus reticulate* Blanco cv. Shatangju) were used as model fruits to evaluate the fungicidal activity of the TBZ suspension concentrate (TBZ-SC, 500 mg L^{-1}) and IL-TBZ (500 mg L^{-1}). The citrus fruits with uniform maturity and size were selected and washed with water. The stock solutions of two formulations were prepared by dispersing in acetone at a concentration of 500 mg L^{-1}, and the acetone was also treated as a control. Each citrus fruit was wounded with a steel rod to make a 4 mm wide and 3 mm deep wound, and a 10 μL aliquot of mixed spore suspension containing 10^6 conidia/mL of *Penicillium italicum* was injected into each wound with a pipette. The fruits were treated by dipping in 500 mg L^{-1} of TBZ-SC and IL-TBZ for 1 min. The experimental design was completely randomized with three replicates, each replicate was 50 fruits maintained under 28 °C, and different relative humidity environments (10, 25, 38, and 50% r.h.) were applied. The disease index was assessed by investigating the number of mildewy fruits at 1, 3, 5, and 10 d after treatment.

$$\text{Disease index} = \frac{\text{The number of mildewy fruits}}{50} \times 100\%$$

2.7. Acute Toxicity to *Danio rerio*. In order to estimate the acute toxicity of TBZ-SC and IL-TBZ to fish, zebrafish (*Danio rerio*) which have been a prominent model vertebrate in a variety of disciplines was selected as a typical environment monitoring aquatic animals in this study.[48] The fish were cultured for 2 weeks using dechlorinated water (temperature 26 ± 1 °C, pH 7.2 ± 0.2) with oxygen saturation >70% and 12 h photophase before performing the experiment. After acclimatization, fish were exposed to different concentrations of TBZ-SC and IL-TBZ (0.8, 1.6, 3.2, 6.4, 12.8, and 25.6 mg L^{-1}) for 96 h with the untreated group as control. The experimental design was completely randomized with three replicates, and each replicate was 10 fish. All the treatments were monitored daily to estimate the acute toxicity of the TBZ and IL-TBZ to fish.

3. RESULTS AND DISCUSSION

3.1. Preparation and Characterization of IL-TBZ. The structures of all the synthesized compounds were characterized by ^{1}H NMR spectroscopy and elemental analysis. ^{1}H NMR data of Ia, Ib, and IL-TBZ are summarized in Table 2. In ^{1}H NMR spectroscopy, Ia presented the disappearance of the secondary amine (−NH−) peak and the appearance of a methylene group ($-CH_2-$) peak located at 4.87 ppm. Ib

https://doi.org/10.1021/acsomega.2c07511
ACS Omega 2023, 8, 3484−3492

Table 2. ^{1}H NMR Data of the Compounds

compound	δ (ppm)
IL	^{1}H NMR (300.13 MHz; DMSO-d_6; Me_4Si) δ ppm = 10.19 (s, 1H, CH), 8.22 (d, J = 6.42 Hz, 2H, CH), 8.47 (d, J = 6.27 Hz, 2H, CH), 4.43 (s, 3H, CH_3)
Ia	^{1}H NMR (300.13 MHz; DMSO-d_6; Me_4Si) δ ppm = 11.83 (d, J = 3.00 Hz, 1H, CH), 9.06 (d, J = 3.00 Hz, 1H, CH), 8.50 (m, 1H, CH), 7.90 (m, 1H, CH), 7.53 (m, 2H, CH), 4.87 (s, 2H, CH_2)
Ib	^{1}H NMR (300.13 MHz; DMSO-d_6; Me_4Si) δ ppm = 9.11 (s, 1H, CH), 8.13 (s, 1H, CH), 7.59 (d, J = 5.46 Hz, 2H, CH), 7.22 (m, 2H, CH), 3.66 (s, 2H, CH_2), 3.47 (t, J = 6.36 Hz, 2H, CH_2), 2.74 (t, J = 4.78 Hz, 2H, CH_2)
IL-TBZ	^{1}H NMR (300.13 MHz; DMSO-d6; Me_4Si) δ ppm = 9.31 (s, 1H, CH), 9.08 (d, J = 7.63 Hz, 2H, CH), 8.09 (s, 1H, CH), 7.88 (d, J = 4.05 Hz, 2H, CH), 7.62 (d, J = 5.13 Hz, 1H, CH), 7.48 (d, J = 3.21 Hz, 1H, CH), 7.33 (m, 2H,CH), 6.56 (s, 1H, CH), 4.36 (s, 3H,CH_3), 3.63 (m, 4H, CH_2), 2.69 (t, J = 5.71 Hz, 2H, CH_2)

presented two triple peaks of methylene groups (−CH_2−) located at 3.47 and 2.74 ppm. A single peak of the aldehyde group (−CH═O) located at 10.19 ppm of IL shifted upfield to 6.56 ppm attributed to C−H of IL-TBZ, and the increased number of hydrogen atoms demonstrated that the IL-TBZ was successfully prepared.

3.2. Control Release Behaviors of IL-TBZ. The mechanism of TBZ-triggered release from IL-TBZ is shown in Scheme 2. The IL-TBZ contained hemiacetal and amide bonds are easily broken by water and amidase to trigger the release of TBZ. In order to confirm the release mechanism, the release behaviors under different conditions were investigated, and the results are illustrated in Figure 1.

Scheme 2. Graphical Representation of TBZ-Triggered Release from IL-TBZ by Water and Amidase

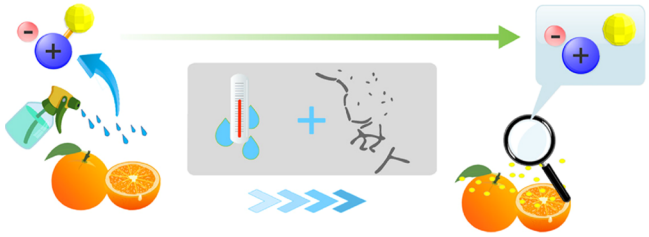

3.2.1. Effect of Different Humidity Conditions. Figure 1A shows the cumulative TBZ release from IL-TBZ in release media at different humidity levels. The results illustrated that the release of the TBZ was triggered by humidity. The cumulative release reached 100% after 480 min when the humidity was 50%, and the cumulative release was reduced with the reduction of humidity. The reason for the above result is that the hemiacetal is sensitive to water and can be easily broken, and the amide bond of IL-TBZ could be hydrolyzed under the presence of appropriate amidase; simultaneously, the active ingredient released depended on the amount of water in the environment.[32,49] The release behaviors of IL-TBZ that respond to water as release triggers for the pesticide were discussed and evaluated, demonstrating the control of release dependent on the presence of amidase and amount of water available.

3.2.2. Effect of Different pH Values. The release behaviors of the IL-TBZ under different pH values at 38% humidity are illustrated in Figure 1B. The TBZ could not be detected in the 38% humidity release medium at pH 7.5 but could be obviously detected at the acidic release system. Besides, the release behaviors were also influenced by the pH values of the environment. After 480 min, the cumulative release was more than 75% at pH 4.5, but was below 50% at pH 5.5 and 6.5, which demonstrated that the cumulative release of TBZ from IL-TBZ was increased with the reduction of pH values. The main reason for this is that the amide bond could be broken under acid conditions according to the literature.[50] Therefore, it was concluded that an acid condition increased the release amount of TBZ, which demonstrated that the IL-TBZ is more suitable for applications in eosinophilic bacteria control.

3.3. Release Kinetics. In order to further study the release regular of IL-TBZ, the cumulative release rates were fitted by the Korsmeyer−Peppas model, zero-order model, first-order model, Hixson−Crowell model, Weibull model, Higuchi model, logistic model, and quadratic model equations. The nonlinear fitting curves of IL-TBZ under different humidity conditions and pH values are illustrated in Figure 2. The different parameters of release models shown in Table 3 were calculated by different equations, and r^2 was used to determine

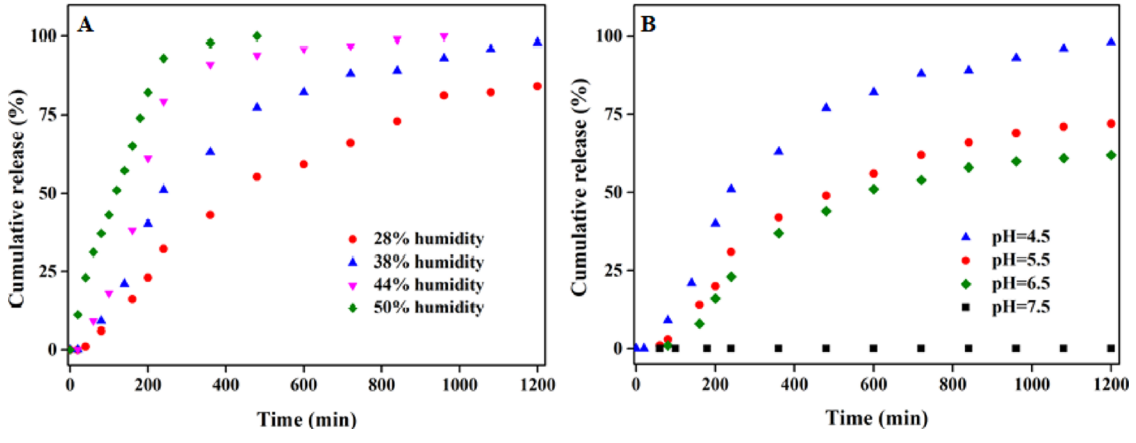

Figure 1. Effect of different humidity (A) and pH values (B) and amidase on the release behaviors of TBZ from IL-TBZ.

https://doi.org/10.1021/acsomega.2c07511
ACS Omega 2023, 8, 3484−3492

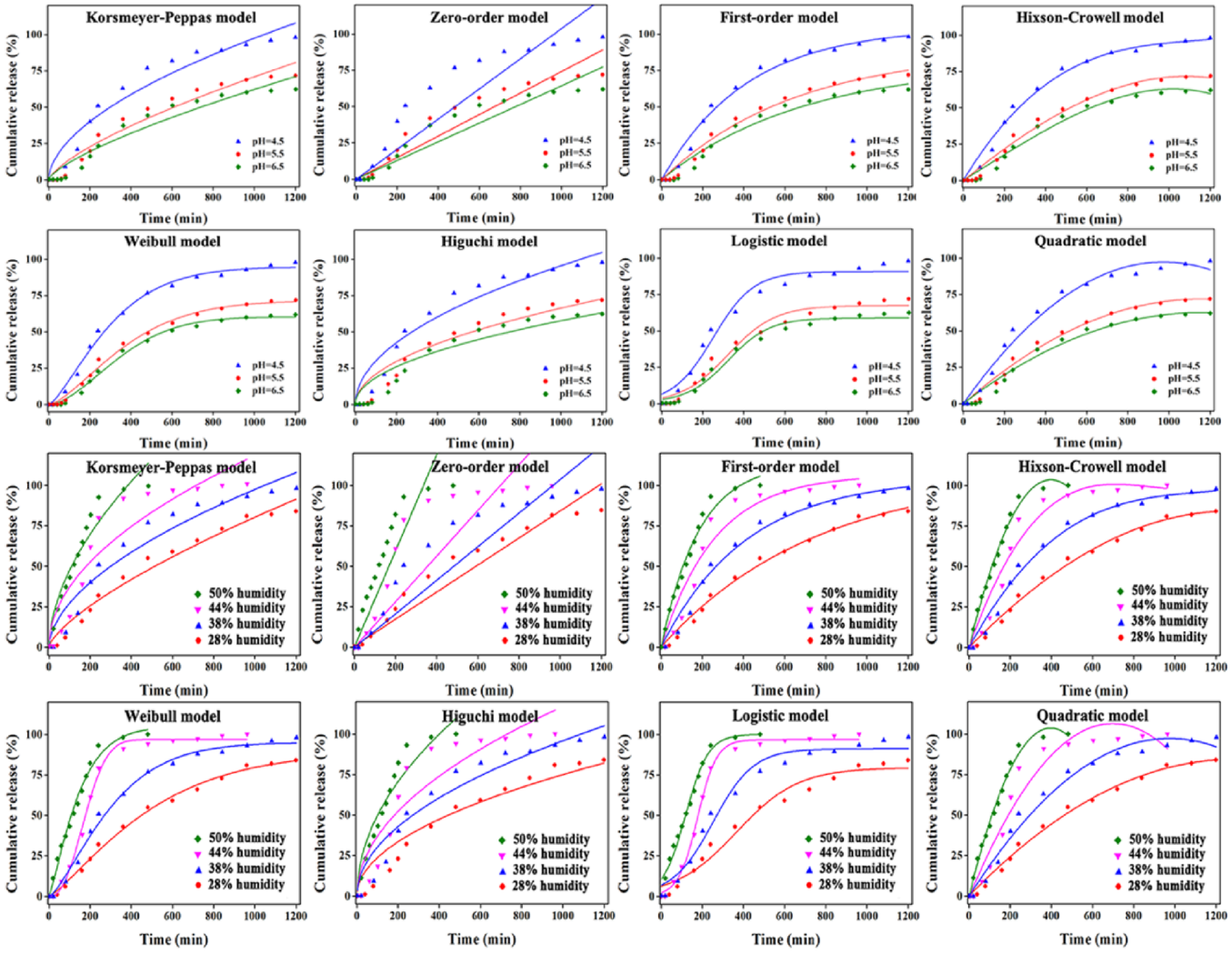

Figure 2. Release curves of IL-TBZ under different humidity levels and pH values.

the suitability of each release models. The results illustrated that the r^2 under different release conditions fitted by the Weibull model were all >0.99, which demonstrated that the Weibull model was a more suitable release model for IL-TBZ.

3.4. Bioactivity. Figure 3 shows the effect of TBZ and IL-TBZ in the disease index of *Citrus reticulate*, which was investigated by calculating the number of mildewy fruits under different humidity conditions. Compared with few mildewy fruits after treating by TBZ, about 11 and 44% of mildewy fruits were found at 1st and 3rd day after treating by IL-TBZ under 10% humidity condition (Figure 3a). However, according to Figure 3b, the number of mildewy fruits treated by TBZ were 20% more than that treated by IL-TBZ at 3rd day under 25% humidity condition and increased over time. The high humidity environment provided suitable conditions for fungal infection. Meanwhile, this was also mainly because the release of active ingredients from IL-TBZ depended on the humidity of the environment which could break the hemiacetal of IL-TBZ and accumulated the release of active ingredients that increased with the increase of time.[32] The results from Figure 3b,d clearly illustrated that the disease index treated by IL-TBZ was lower than that treated by TBZ under 38 and 50% humidity environments, and the disease index treated by IL-TBZ decreased with humidity increase. However, on the contrary, the disease index by TBZ was increased with humidity increase. The mildewy symptoms of the *Citrus reticulate* after 5 and 10 days treated by control (a), TBZ (b), and IL-TBZ (c) under 50% humidity are illustrated in Figure 4. These were probably attributed to the enzyme and humidity dual-triggered properties, and then, the active ingredients could release from IL-TBZ responsively. The hemiacetal of IL-TBZ could be broken by moisture from humidity of the environment, and the amide bond of IL-TBZ could be broken by the enzyme and acidic conditions. *Penicillium italicum* acidified the ambient environments of citrus fruits during decay development and reduced the host pH by 0.5−1.0 units.[51] The amidase applied to triggered-release TBZ was produced by antagonistic bacteria located on the surface of fruits.[52,53] Therefore, the dual-triggered IL-TBZ exhibited good antifungal efficacy against *Penicillium italicum* than TBZ under high humidity environments.

3.5. Acute Toxicity to *Danio rerio*. The cumulative mortalities of zebrafish exposed to the TBZ and IL-TBZ at different time intervals are illustrated in Figure 5. The results showed that the cumulative mortalities were concentration-dependent and time-dependent for all treatments. The higher concentrations of exposure were the higher the cumulative mortalities were. The longer time of exposure was the higher the cumulative mortalities were. Figure 5d shows that there are no significant cumulative mortalities of zebrafish exposed to 0.8

https://doi.org/10.1021/acsomega.2c07511
ACS Omega 2023, 8, 3484−3492

Table 3. Fitting Results for the Release Curves of IL-TBZ

		pH = 4.5				38% humidity	
release model	parameter	28% humidity	38% humidity	44% humidity	50% humidity	pH = 5.5	pH = 6.5
Korsmeyer−Peppas model	k_1	0.7122	0.5533	0.5083	0.5562	0.7021	0.7297
	k_2	0.5868	2.1318	3.5100	3.6908	0.5567	0.4008
	r^2	0.9731	0.9308	0.8440	0.9199	0.9501	0.9354
zero-order model	k_1	0.0836	0.1039	0.1412	0.2976	0.07412	0.0643
	r^2	0.9741	0.9369	0.8891	0.9142	0.9611	0.9582
first-order model	k_1	108.5315	104.5842	106.6383	113.8042	88.8331	79.7928
	k_2	0.0013	0.0024	0.0038	0.0055	0.0016	0.0015
	r^2	0.9917	0.9853	0.9500	0.9821	0.9814	0.9698
Hixson−Crowell model	k_1	0.1302	0.2347	0.3648	0.5268	0.1174	0.0884
	k_2	-4.7525×10^{-5}	-1.9892×10^{-5}	-4.2932×10^{-4}	-6.8442×10^{-4}	-3.3239×10^{-5}	7.8320×10^{-5}
	k_3	-2.2675×10^{-9}	5.8931×10^{-8}	1.6205×10^{-7}	3.3453×10^{-8}	-1.3001×10^{-8}	-3.3456×10^{-8}
	r^2	0.9931	0.9881	0.9614	0.9817	0.9862	0.9806
Weibull model	k_1	0.0019	0.0030	0.0049	0.0065	0.0024	0.0025
	k_2	1.2418	1.3481	2.3650	1.2287	1.4477	1.7167
	k_3	89.3446	94.9552	96.7576	104.6033	71.4579	60.4298
	r^2	0.9954	0.9937	0.9966	0.9918	0.9940	0.9949
Higuchi model	k_1	2.3711	3.0271	3.6972	4.9975	2.0964	1.8110
	r^2	0.9224	0.9257	0.8438	0.9119	0.9027	0.8786
logistic model	k_1	11.6418	12.8964	44.6524	8.5128	16.3330	24.2883
	k_2	0.0067	0.0102	0.0216	0.0181	0.0087	0.0099
	k_3	79.4728	90.7758	96.6511	99.9262	67.3614	58.3266
	r^2	0.9728	0.9765	0.9866	0.9849	0.9755	0.9838
quadratic model	k_1	0.1315	0.2001	0.3063	0.5242	0.1249	0.1077
	k_2	-5.1210×10^{-5}	-1.0284×10^{-4}	-2.2021×10^{-4}	-6.6335×10^{-4}	-5.4313×10^{-4}	-4.6399×10^{-4}
	r^2	0.9931	0.9821	0.9513	0.9898	0.9858	0.9770

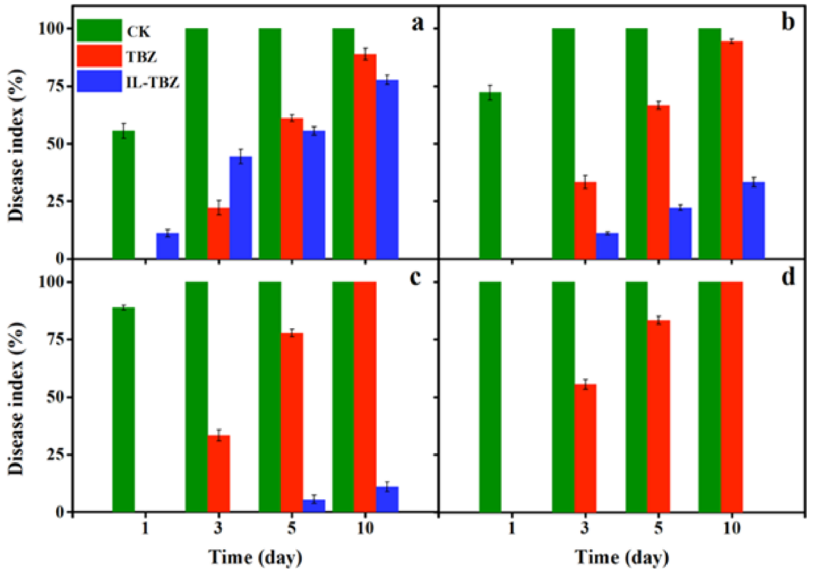

Figure 3. Effect of different treatments on the disease index of *Citrus reticulate* under 10% humidity (a), 25% humidity (b), 38% humidity (c), and 50% humidity (d).

and 1.6 mg L^{-1} of TBZ after 96 h. However, the cumulative mortalities of treatment with 3.2, 6.4, 12.8, and 25.6 mg L^{-1} of TBZ obviously rose to 33.33, 80, 100, and 100%, respectively. Compared with exposure of TBZ, there are no obvious cumulative mortalities of zebrafish exposed to 0.8, 1.6, 3.2, and 6.4 mg L^{-1} of IL-TBZ after 96 h. In addition, 23.33 and 30% of cumulative mortalities on zebrafish was observed when exposed to 12.8 and 25.6 mg L^{-1} of IL-TBZ after 96 h, respectively.

To intuitively evaluate the toxicity of the TBZ and IL-TBZ to zebrafish, the median lethal concentration (LC_{50}) values and 95% confidence intervals were calculated according to the method of the literature,[54] and results are listed in Table 4. The 96 h LC_{50} of IL-TBZ was 25.02 mg L^{-1}, which was almost 6 times higher than 4.13 mg L^{-1} of the TBZ. The LC_{50} values of TBZ between 1 and 10 mg L^{-1} were considered highly toxic, and the LC_{50} values of IL-TBZ between 10 and 100 mg L^{-1} were considered moderately toxic.[55] The results demonstrated

https://doi.org/10.1021/acsomega.2c07511
ACS Omega 2023, 8, 3484−3492

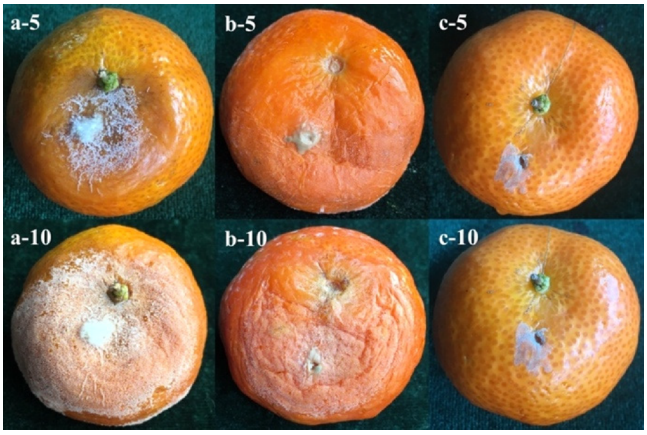

Figure 4. Mildewy symptoms of the *Citrus reticulate* after 5 and 10 days treated by control (a-5 and a-10), TBZ (b-5 and b-10), and IL-TBZ (c-5, and c-10) under 50% humidity.

that the reduced acute toxicity of IL-TBZ could decrease the threats caused by TBZ to aquatic organisms.

4. CONCLUSIONS

In this work, the novel prodrug (IL-TBZ) based on IL was prepared by forming the hemiacetal between the hydroxy of derivatized TBZ and the aldehyde of IL. On the basis of this novel design, the TBZ released from IL-TBZ was triggered by water and enzymes and depended on the amount of water available and the own existent antagonistic bacteria of fruits. The results showed that the prodrug had remarkable triggered release under different pH, humidity, and enzyme conditions, as well as low toxicity to aquatic organisms. This release system may be extended to other pesticides which were used in a humid environment, especially in the application of mildew-proof and dampproof.

Table 4. Median Lethal Concentration (LC_{50}) Values, 95% Confidence Intervals of TBZ and IL-TBZ in Zebrafish

	TBZ		IL-TBZ	
exposure time (h)	LC_{50} (mg L^{-1})	95% confidence interval	LC_{50} (mg L^{-1})	95% confidence interval
24	9.48	6.72−13.37	36.20	
48	6.70	4.86−9.24	33.78	29.70−38.43
72	5.44	3.99−7.49	28.74	22.30−35.91
96	4.13	3.16−5.38	25.02	19.14−32.70

AUTHOR INFORMATION

Corresponding Author

Yongsong Cao − *College of Plant Protection, China Agricultural University, Beijing 100094, China*; Email: caoysong@126.com, caoys@cau.edu.cn

Authors

Wenbing Zhang − *College of Horticulture and Plant Protection, Inner Mongolia Agricultural University, Hohhot 010018, China*; orcid.org/0000-0002-3814-4187

Yan Guo − *College of Horticulture and Plant Protection, Inner Mongolia Agricultural University, Hohhot 010018, China*

Jiale Yang − *College of Horticulture and Plant Protection, Inner Mongolia Agricultural University, Hohhot 010018, China*

Gang Tang − *College of Plant Protection, China Agricultural University, Beijing 100094, China*

Jian Zhang − *College of Horticulture and Plant Protection, Inner Mongolia Agricultural University, Hohhot 010018, China*

Complete contact information is available at: https://pubs.acs.org/10.1021/acsomega.2c07511

Notes

The authors declare no competing financial interest.

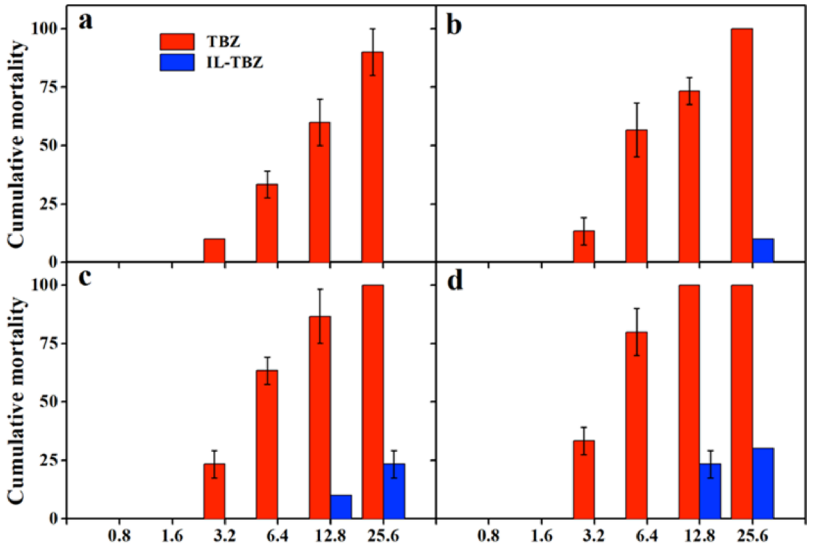

Figure 5. Cumulative mortalities of zebrafish at 24 h (a), 48 h (b), 72 h (c), and 96 h (d) after acute exposure to TBZ and IL-TBZ. All treatments were analyzed in three replicates, whose average data were illustrated by the columns. Error bar was used to represent the standard deviation (SD) of the mean values.

https://doi.org/10.1021/acsomega.2c07511
ACS Omega 2023, 8, 3484−3492

■ ACKNOWLEDGMENTS

This work was supported by the Research Start-up Funds for High-level Researchers in Inner Mongolia Agricultural University (NDYB2019-02), Natural Science Foundation of Inner Mongolia Autonomous Region (2020BS03033), and Program for Young Talents of Science and Technology in Universities of Inner Mongolia Autonomous Region (NJYT23128).

■ REFERENCES

(1) Meissle, M.; Mouron, P.; Musa, T.; Bigler, F.; Pons, X.; Vasileiadis, V. P.; Otto, S.; Antichi, D.; Kiss, J.; Pálinkás, Z.; et al. Pests, pesticide use and alternative options in European maize production: current status and future prospects. *J. Appl. Entomol.* **2010**, *134*, 357−375.

(2) Kaziem, A. E.; Gao, Y.; Zhang, Y.; Qin, X.; Xiao, Y.; Zhang, Y.; You, H.; Li, J.; He, S. α-Amylase triggered carriers based on cyclodextrin anchored hollow mesoporous silica for enhancing insecticidal activity of avermectin against *Plutella xylostella*. *J. Hazard. Mater.* **2018**, *359*, 213−221.

(3) Liu, B.; Wang, Y.; Yang, F.; Wang, X.; Shen, H.; Cui, H.; Wu, D. Construction of a controlled-release delivery system for pesticides using biodegradable PLA-based microcapsules. *Colloids Surf., B* **2016**, *144*, 38−45.

(4) Huang, B.; Chen, F.; Shen, Y.; Qian, K.; Wang, Y.; Sun, C.; Zhao, X.; Cui, B.; Gao, F.; Zeng, Z.; Cui, H. Advances in targeted pesticides with environmentally responsive controlled release by nanotechnology. *Nanomaterials* **2018**, *8*, 102.

(5) Zhao, X.; Cui, H.; Wang, Y.; Sun, C.; Cui, B.; Zeng, Z. Development strategies and prospects of nano-based smart pesticide formulation. *J. Agric. Food Chem.* **2018**, *66*, 6504−6512.

(6) Athanassiou, C. G.; Kavallieratos, N. G.; Benelli, G.; Losic, D.; Usha Rani, P.; Desneux, N. Nanoparticles for pest control: current status and future perspectives. *J. Pest Sci.* **2018**, *91*, 1−15.

(7) Benelli, G.; Pavela, R.; Maggi, F.; Petrelli, R.; Nicoletti, M. Commentary: making green pesticides greener? The potential of plant products for nanosynthesis and pest control. *J. Cluster Sci.* **2017**, *28*, 3−10.

(8) Feng, J.; Ma, Y.; Chen, Z.; Liu, Q.; Yang, J.; Gao, Y.; Chen, W.; Qian, K.; Yang, W. Development and characterization of pyriproxyfen-loaded nanoemulsion for housefly control: improving activity, reducing toxicity, and protecting ecological environment. *ACS Sustainable Chem. Eng.* **2021**, *9*, 4988−4999.

(9) Li, M.; Xu, W.; Hu, D.; Song, B. Preparation and application of pyraclostrobin microcapsule formulations. *Colloids Surf., A* **2018**, *553*, 578−585.

(10) Xiang, Y.; Zhang, G.; Chen, C.; Liu, B.; Cai, D.; Wu, Z. Fabrication of a pH-responsively controlled-release pesticide using an attapulgite-based hydrogel. *ACS Sustainable Chem. Eng.* **2017**, *6*, 1192−1201.

(11) Kumar, S.; Bhanjana, G.; Sharma, A.; Sidhu, M. C.; Dilbaghi, N. Synthesis, characterization and on field evaluation of pesticide loaded sodium alginate nanoparticles. *Carbohydr. Polym.* **2014**, *101*, 1061−1067.

(12) Zhang, W.; He, S.; Liu, Y.; Geng, Q.; Ding, G.; Guo, M.; Deng, Y.; Zhu, J.; Li, J.; Cao, Y. Preparation and characterization of novel functionalized prochloraz microcapsules using silica-alginate-elements as controlled release carrier materials. *ACS Appl. Mater. Interfaces* **2014**, *6*, 11783−11790.

(13) Samadzadeh, M.; Boura, S. H.; Peikari, M.; Kasiriha, S. M.; Ashrafi, A. A review on self-healing coatings based on micro/nanocapsules. *Prog. Org. Coat.* **2010**, *68*, 159−164.

(14) Lertsutthiwong, P.; Rojsitthisak, P.; Nimmannit, U. Preparation of turmeric oil-loaded chitosan-alginate biopolymeric nanocapsules. *Mater. Sci. Eng., C* **2009**, *29*, 856−860.

(15) Irwin, W. J.; Belaid, K. A.; Alpar, H. O. Drug-delivery by ion-exchange: part IIII: interaction of ester pro-drugs of propranolol with cationic exchange resins. *Drug Dev. Ind. Pharm.* **1987**, *13*, 2047−2066.

(16) Sagnella, S. M.; Gong, X.; Moghaddam, M. J.; Conn, C. E.; Kimpton, K.; Waddington, L. J.; Krodkiewska, I.; Drummond, C. J. Nanostructured nanoparticles of self-assembled lipid pro-drugs as a route to improved chemotherapeutic agents. *Nanoscale* **2011**, *3*, 919−924.

(17) Müller, I. A.; Kratz, F.; Jung, M.; Warnecke, A. Schiff bases derived from p-aminobenzyl alcohol as trigger groups for pH-dependent prodrug activation. *Tetrahedron Lett.* **2010**, *51*, 4371−4374.

(18) Gopin, A.; Pessah, N.; Shamis, M.; Rader, C.; Shabat, D. A chemical adaptor system designed to link a tumor-targeting device with a prodrug and an enzymatic trigger. *Angew. Chem. Int. Ed.* **2003**, *115*, 341−346.

(19) Dai, Y.; Xiao, H.; Liu, J.; Yuan, Q.; Ma, P. A.; Yang, D.; Li, C.; Cheng, Z.; Hou, Z.; Yang, P.; Lin, J. In vivo multimodality imaging and cancer therapy by near-infrared light-triggered trans-platinum pro-drug-conjugated upconverison nanoparticles. *J. Am. Chem. Soc.* **2013**, *135*, 18920−18929.

(20) Peng, H.; Huang, X.; Oppermann, A.; Melle, A.; Weger, L.; Karperien, M.; Wöll, D.; Pich, A. A facile approach for thermal and reduction dual-responsive prodrug nanogels for intracellular doxorubicin delivery. *J. Mater. Chem. B* **2016**, *4*, 7572−7583.

(21) Imai, T.; Hosokawa, M. Prodrug approach using carboxylesterases activity: catalytic properties and gene regulation of carboxylesterase in mammalian tissue. *J. Pestic. Sci.* **2010**, *35*, 229−239.

(22) Liu, Y.; Sun, Y.; He, S.; Zhu, Y.; Ao, M.; Li, J.; Cao, Y. Synthesis and characterization of gibberellin-chitosan conjugate for controlled-release applications. *Int. J. Biol. Macromol.* **2013**, *57*, 213−217.

(23) Liu, Y.; Sun, Y.; Ding, G.; Geng, Q.; Zhu, J.; Guo, M.; Duan, Y.; Wang, B.; Cao, Y. Synthesis, characterization, and application of microbe-triggered controlled-release kasugamycin-pectin conjugate. *J. Agric. Food Chem.* **2015**, *63*, 4263−4268.

(24) Tian, Y.; Zhang, X.; Huang, Y.; Tang, G.; Gao, Y.; Chen, X.; Zhou, Z.; Li, Y.; Li, X.; Wang, H.; et al. Amphiphilic prodrug nanomicelles of fipronil coupled with natural carboxylic acids for improving physicochemical properties and reducing the toxicities to aquatic organisms. *Chem. Eng. J.* **2022**, *439*, No. 135717.

(25) Salgado, V. L.; David, M. D. Chance and design in proinsecticide discovery. *Pest Manage. Sci.* **2017**, *73*, 723−730.

(26) Gordon, C. M.; Holbrey, J. D.; Kennedy, A. R.; Seddon, K. R. Ionic liquid crystals: hexafluorophosphate salts. *J. Mater. Chem.* **1998**, *8*, 2627−2636.

(27) Tang, G.; Liu, Y.; Ding, G.; Zhang, W.; Liang, Y.; Fan, C.; Dong, H.; Yang, J.; Kong, D.; Cao, Y. Ionic liquids based on bromoxynil for reducing adverse impacts on the environment and human health. *New J. Chem.* **2017**, *41*, 8650−8655.

(28) Jaitely, V.; Karatas, A.; Florence, A. T. Water-immiscible room temperature ionic liquids (RTILs) as drug reservoirs for controlled release. *Int. J. Pharm.* **2008**, *354*, 168−173.

(29) Smith, K. B.; Bridson, R. H.; Leeke, G. A. Solubilities of pharmaceutical compounds in ionic liquids. *J. Chem. Eng. Data* **2011**, *56*, 2039−2043.

(30) Goindi, S.; Kaur, R.; Kaur, R. An ionic liquid-in-water microemulsion as a potential carrier for topical delivery of poorly water soluble drug: development, ex-vivo and in-vivo evaluation. *Int. J. Pharm.* **2015**, *495*, 913−923.

(31) Armand, M.; Endres, F.; MacFarlane, D. R.; Ohno, H.; Scrosati, B. Ionic-liquid materials for the electrochemical challenges of the future. *Nat. Mater.* **2009**, *8*, 621.

(32) Gunaratne, H. Q. N.; Nockemann, P.; Seddon, K. R. Pro-fragrant ionic liquids with stable hemiacetal motifs: water-triggered release of fragrances. *Chem. Commun.* **2015**, *51*, 4455−4457.

(33) Banerjee, A.; Ibsen, K.; Brown, T.; Chen, R.; Agatemor, C.; Mitragotri, S. Ionic liquids for oral insulin delivery. *Proc. Natl. Acad. Sci. U. S. A.* **2018**, *115*, 7296−7301.

(34) Cuckler, A. C. Thiabendazole, a new broad spectrum anthelmintic. *J. Parasitol.* **1961**, *47*, 36−37.

https://doi.org/10.1021/acsomega.2c07511
ACS Omega 2023, 8, 3484−3492

(35) D'Aquino, S.; Palma, A.; Angioni, A.; Schirra, M. Residue levels and efficacy of fludioxonil and thiabendazole in controlling postharvest green mold decay in citrus fruit when applied in combination with sodium bicarbonate. *J. Agric. Food Chem.* **2013**, *61*, 296−306.
(36) Dunia, E.; Elisenda Pulido, M.; Cristina Fernández, R.; Ortega, J. A.; Sebastián, O.; José, M. Degradation and detoxification of banana postharvest treatment water using advanced oxidation techniques. *Green Sustainable Chem.* **2011**, *1*, 7067.
(37) Oh, S. J.; Park, J.; Lee, M. J.; Park, S. Y.; Lee, J. H.; Choi, K. Ecological hazard assessment of major veterinary benzimidazoles: acute and chronic toxicities to aquatic microbes and invertebrates. *Environ. Toxicol. Chem.* **2006**, *25*, 2221−2226.
(38) Plater, M. J.; Barnes, P.; McDonald, L. K.; Wallace, S.; Archer, N.; Gelbrich, T.; Horton, P. N.; Hursthouse, M. B. Hidden signatures: new reagents for developing latent fingerprints. *Org. Biomol. Chem.* **2009**, *7*, 1633−1641.
(39) Wang, L.; Hu, Y.; Hao, Y.; Li, L.; Zheng, C.; Zhao, H.; Niu, M.; Yin, Y.; Zhang, Z.; Zhang, Y. Tumor-targeting core-shell structured nanoparticles for drug procedural controlled release and cancer sonodynamic combined therapy. *J. Controlled Release* **2018**, *286*, 74−84.
(40) Polli, J. E.; Rekhi, G. S.; Augsburger, L. L.; Shah, V. P. Methods to compare dissolution profiles and a rationale for wide dissolution specifications for metoprolol tartrate tablets. *J. Pharm. Sci.* **1997**, *86*, 690−700.
(41) Sood, A.; Panchagnula, R. Role of dissolution studies in controlled release drug delivery systems. *STP Pharma Sci.* **1999**, *9*, 157−168.
(42) Yuksel, N.; Kanık, A. E.; Baykara, T. Comparison of in vitro dissolution profiles by ANOVA-based, model-dependent and-independent methods. *Int. J. Pharm.* **2000**, *209*, 57−67.
(43) Lu, D. R.; Abu-Izza, K.; Mao, F. Nonlinear data fitting for controlled release devices: an integrated computer program. *Int. J. Pharm.* **1996**, *129*, 243−251.
(44) Koizumi, T.; Ritthidej, G. C.; Phaechamud, T. Mechanistic modeling of drug release from chitosan coated tablets. *J. Controlled Release* **2001**, *70*, 277−284.
(45) Murali Mohan Babu, G. V.; Prasad, C. S.; Hima Sankar, K.; Narayan, C. P.; Ramana Murthy, K. V. Evaluation of gum karaya as a carrier in the design of oral controlled-release hydrophilic matrix systems. *Acta Pharm.* **2001**, *51*, 273−287.
(46) Su, X. Y.; Al-Kassas, R.; Li Wan Po, A. Statistical modelling of ibuprofen release from spherical lipophilic matrices. *Eur. J. Pharm. Biopharm.* **1994**, *40*, 73−76.
(47) Costa, P.; Lobo, J. M. S. Modeling and comparison of dissolution profiles. *Eur. J. Pharm. Sci.* **2001**, *13*, 123−133.
(48) Hill, A. J.; Teraoka, H.; Heideman, W.; Peterson, R. E. Zebrafish as a model vertebrate for investigating chemical toxicity. *Toxicol. Sci.* **2005**, *86*, 6−19.
(49) Candel, I.; Aznar, E.; Mondragón, L.; de la Torre, C.; Martínez-Máñez, R.; Sancenón, F.; Marcos, M. D.; Amorós, P.; Guillem, C.; Pérez-Payá, E.; Costero, A.; Gil, S.; Parra, M. Amidase-responsive controlled release of antitumoral drug into intracellular media using gluconamide-capped mesoporous silica nanoparticles. *Nanoscale* **2012**, *4*, 7237−7245.
(50) He, S.; Zhang, W.; Li, D.; Li, P.; Zhu, Y.; Ao, M.; Li, J.; Cao, Y. Preparation and characterization of double-shelled avermectin microcapsules based on copolymer matrix of silica-glutaraldehyde-chitosan. *J. Mater. Chem. B* **2013**, *1*, 1270−1278.
(51) Prusky, D.; McEvoy, J. L.; Saftner, R.; Conway, W. S.; Jones, R. Relationship between host acidification and virulence of *Penicillium spp*. on apple and citrus fruit. *Phytopathology* **2004**, *94*, 44−51.
(52) Arrebola, E.; Sivakumar, D.; Korsten, L. Effect of volatile compounds produced by Bacillus strains on postharvest decay in citrus. *Biol. Control* **2010**, *53*, 122−128.
(53) Obagwu, J.; Korsten, L. Integrated control of citrus green and blue molds using *Bacillus subtilis* in combination with sodium bicarbonate or hot water. *Postharvest Biol. Technol.* **2003**, *28*, 187−194.
(54) Hamilton, M. A.; Russo, R. C.; Thurston, R. V. Trimmed Spearman-Karber method for estimating median lethal concentrations in toxicity bioassays. *Environ. Sci. Technol.* **1977**, *11*, 714−719.
(55) Passino, D. R. M.; Smith, S. B. Acute bioassays and hazard evaluation of representative contaminants detected in great lakes fish. *Environ. Toxicol. Chem.* **1987**, *6*, 901−907.

https://doi.org/10.1021/acsomega.2c07511
ACS Omega 2023, 8, 3484−3492